Nanoscale

Accepted Manuscript

Volume 8 | Number 1 | 7 January 2016 | Pages 1–660

Nanoscale

www.rsc.org/nanoscale

ISSN 2040-3364

ROYAL SOCIETY OF CHEMISTRY

PAPER
Qian Wang et al.
TiC₂: a new two-dimensional sheet beyond MXenes

NCNST

ROYAL SOCIETY OF CHEMISTRY

rsc.li/nanoscale

Journal Name

COMMUNICATION

CdS-coated TiO₂ nanotube layers: downscaling tube diameter towards efficient heterostructured photo-electrochemical conversion

M. Krbal, J. Prikryl, R. Zazpe, H. Sopha and J. M. Macak[*]

Novel heterostructured solar cell based on TiO₂ nanotube layers uniformly coated by CdS thin layer (using ALD) is presented. Downscaling the nanotube diameter (95 to 35nm) enhanced twice the UV and VIS light photocurrents. Further photocurrent improvement resulted from prior annealing of TiO₂ nanotube layers from 300 to 600°C.

Ever increasing demand for the long-term replacement of fossil fuels by low-cost, high-efficient, renewable and environmentally friendly sources of energy led photovoltaic technologies encounter a tremendous development to meet this target. Next to silicon[1,2] and chalcogenide[3-5] solar cells, recently new types of thin film-based devices employing TiO₂ mesoporous structures sensitized with organic dyes[6], perovskites[7] and quantum dots[8-10] have been designed and developed. For such devices, the main challenge is to select an appropriate TiO₂ and chromophore couple. However, it was shown that controlling the TiO₂ - chromophore interface increases the efficiency of the cells.[6,11] Such enhancement can be achieved by increasing the interfacial surface area between the chromophore and the TiO₂ in order to facilitate efficient charge separation. Unlike mesoporous TiO₂ supports, ordered nanostructures, such as high aspect ratio self-organized TiO₂ nanotube layers[12,13] or TiO₂ nanorods[14,15] offer the advantage of directed charge transport and controlled phase separation between donor and acceptor parts of the solar cell and thus they seem very promising for nanoscale solar hybrid technologies.[16,17]

In the case of 1D self-organized TiO₂ nanostructures, the overall surface can be easily increased by prolonging their length or reducing their diameters while increasing their number. Especially self-organized TiO₂ nanotube layers possess inner and outer surfaces of tubes which is highly beneficial in comparison with nanowires[18] or nanorods.[14,15] To achieve higher power conversion efficiency levels the surface area can be in the further step coated by secondary material

using chemical bath deposition,[8,19] spincoating,[20,21] sputtering,[22] electrodeposition,[23] a solvothermal method[24,25] and atomic layer deposition (ALD).[26-28] However, only ALD technique is capable to cover homogeneously nanotube interiors as well as exteriors[27,28] and thus ensure best possible TiO₂ - chromophore interface, especially for high-aspect ratio nanotubes.

Herein, we present photo-electrochemical and structural characterization of a new type of heterostructured photochemical half-cells, fabricated using highly ordered n-type conductive TiO₂ nanotubular scaffolds with different diameters (35, 56, 95 nm) coated by CdS (40 cycles, thickness ~6 nm) deposited via a tailored ALD process.

The TiO₂ nanotube layers used in our experiments were prepared by anodization of Ti foils. The anodization conditions for these layers with similar thicknesses and different nanotube inner diameters were described previously.[19] Prior to deposition of CdS, amorphous nanotube layers were converted to anatase/rutile modifications by the annealing protocol applied previously[29] in the range of temperatures from 300 to 600 °C.

In the second step, TiO₂ nanotube layers were coated for the first time by CdS by ALD (TFS200, Beneq) using following conditions. The dimethylcadmium (electronic grade 99.999%) and gaseous H₂S were used as the cadmium precursor and the sulphur source, respectively. High purity nitrogen (99.9999%) was the carrier and purging gas at a flow rate of 400 standard cubic centimetres minute (sccm). Under these deposition conditions, one growth ALD cycle was defined by the following sequence: dimethylcadmium pulse (400ms)-N₂ purge (10s)-H₂S pulse (1s)-N₂ purge (15s). The TiO₂ nanotube layers were CdS-coated at 150 °C applying 40 ALD cycles. This corresponds to the nominal thickness of approx. 6 nm, as confirmed by variable angle spectroscopic ellipsometry (VASE® ellipsometer, J.A. Woollam, Co., Inc.) of CdS coatings on Si wafers. The composition of CdS deposited by ALD on a Si wafer was verified using XPS which showed the Cd:S ratio to be 1:1. The morphology of the TiO₂ nanotube layers were characterized by a field-emission SEM (FE SEM JEOL JSM 7500F) and a high

*Center of Materials and Nanotechnologies, Faculty of Chemical Technology, University of Pardubice, Nam. Cs. Legii 565, 530 02 Pardubice, Czech Republic
*Corresponding author: email jan.macak@upce.cz, phone +420466037401
See DOI: 10.1039/x0xx00000x*

COMMUNICATION Journal Name

resolution TEM (HRTEM, FEI Titan) equipped with STEM mode and EDX mapping.

Fig. 1 shows top-view SEM images of blank TiO_2 annealed (400°C) nanotube layers with different average nanotube diameters: A) 35 nm, B) 56 nm, C) 95 nm. The SEM images D-F represent top-view images of corresponding TiO_2 nanotube layers coated with CdS by ALD. One can see an obvious increase of the wall thicknesses and thus smaller inner nanotube diameters between blank and coated nanotube layers which unequivocally indicates on the presence of the CdS coating. In order to demonstrate that the TiO_2 nanotube layers with different diameters are homogeneously coated with CdS throughout the whole thickness of all layers (approx. 600 nm), cross-sectional SEM analyses of CdS coated nanotube layers were carried out. These analyses verified that the nanotubes are indeed well coated from the top to the bottom part and as well within interiors and exteriors for all nanotube layers. Representative cross-sectional SEM images are shown as insets in Fig. 1.
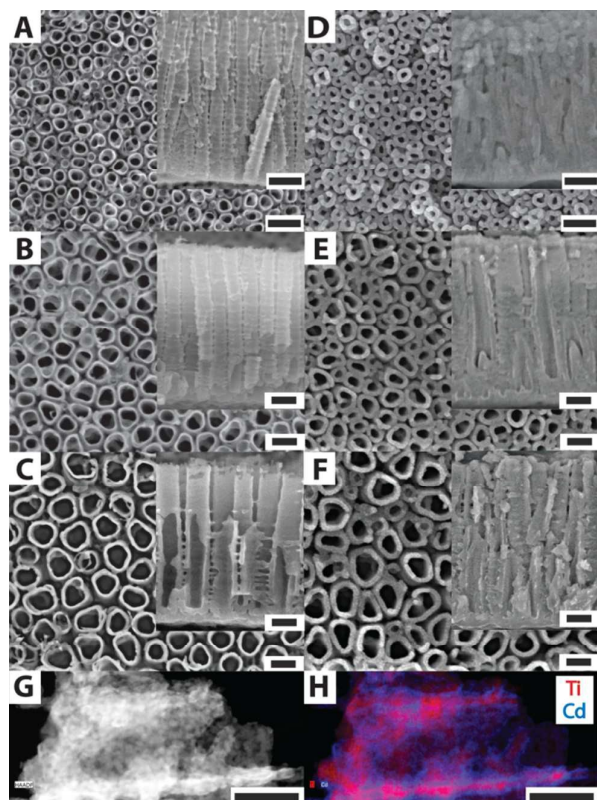

Fig. 1 SEM top-view images of self-organized TiO_2 nanotube layers with different average nanotube diameters annealed at 400°C: A) 35 nm, B) 56 nm, C) 95 nm. SEM images D-F represent top-view images of corresponding TiO_2 nanotube layers coated with CdS by ALD. Cross-section SEM images of corresponding TiO_2 nanotube layers and CdS-coated counterparts are shown as insets. G) STEM image of a fragment of CdS-coated TiO_2 nanotube, H) EDX map of the corresponding STEM image showing Cd and Ti distribution. All scale bars show the distance of 100 nm.

Fig. 1 G and H show STEM image and EDX map, respectively, of the CdS-coated nanotube shown in Fig. 1 F. Evidently, the Cd species (forming CdS) are present all along the TiO_2 nanotube, in line with the expectation of uniform ALD coating.[27,28]

It was supposed that the significant increase of the number of nanotubes per cm^2 may have the potential to enhance the photocurrent response of heterostructured solar cells due to the increase of the interfacial surface area between the chromophore (produced as conformal coating by ALD) and the TiO_2 nanotube layers. The estimated overall surface areas by simple calculations per 1 cm^2 of TiO_2 nanotube layer for the used TiO_2 nanotube layers are: 52, 29 and 23 cm^2 / cm^2 of the macroscopic geometrical area for 35, 56 and 95 nm inner diameters of TiO_2 nanotubes, respectively.

In order to obtain information about the photo-electrochemical properties of the nanotube layers and the CdS-coated TiO_2 nanotube layer heterostructures, photocurrent measurements were carried out in an aqueous electrolyte containing 0.1 M Na_2SO_4, employing a photoelectric spectrophotometer (Instytut Fotonowy) in the wavelength range 300 – 650 nm at 0.4 V vs Ag/AgCl reference electrode.[21] Apparently, the coupling of CdS coatings with TiO_2 nanotube layers causes a strong sensitizing effect, as shown in Fig. 2. Firstly, the photocurrent density under UV light is enhanced several times as compared to blank TiO_2 nanotube layers. We believe that this phenomenon is related to the annihilation of surface states during ALD of CdS which significantly improves the charge collection efficiency, as demonstrated in previous works.[20,21,30,31] More importantly, a robust photocurrent density can be observed in the visible spectral range, peaking at a wavelength of 470 nm. The recorded incident photon-to-electron conversion efficiencies (IPCE) that are shown in Fig. 2B are significantly higher than values reported previously for chalcogenide sensitized TiO_2 nanotube layers by chemical bath deposition,[8,19] spincoating[20,21] and electrodeposition,[22] due the fact that the ALD coating of CdS leads to the largest possible interfacial contact area with TiO_2 nanotube layers from these techniques.
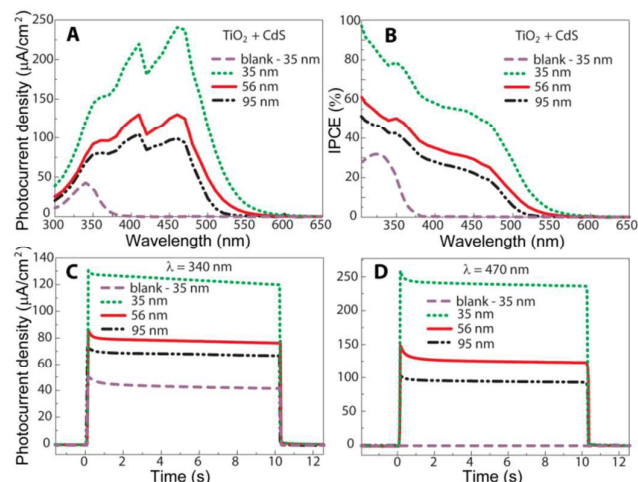

Fig. 2 A) photocurrent density B) incident photon-to-electron conversion efficiency C) and D) photocurrent transients at 340 nm and 470 nm, respectively, recorded for anatase TiO_2 nanotube layers annealed at 400°C with different diameters sensitized with crystalline CdS films deposited by ALD.

Journal Name

COMMUNICATION

In addition, we found that the collected photocurrent density increased approximately by a factor of 2 with downscaling of the TiO_2 nanotube diameter from 95 to 35 nm in the spectral range from 300 to 500 nm. This result perfectly coincides with the increased active surface area of TiO_2 nanotube layers in the same range of nanotube diameters. Thus, our findings well corroborate with the assumption that an increase of the interfacial surface area between the chromophore and the TiO_2 nanotube layers should generate higher photocurrent density due to a larger amount of the CdS absorber deposited by ALD. Conclusively, the combination of 1D nanostructured TiO_2 nanotube layers with a thin light absorber deposited by ALD opens a door for a new approach for fabrication of efficient novel hybrid solar cells. For the energy diagram of CdS / TiO_2 heterostructure, we refer to previously published literature.[25,32]

Further, we investigated the influence of thermal treatment of uncoated TiO_2 nanotube layers on the photoresponse of subsequently prepared heterostructures based on CdS-coated TiO_2 nanotube layers. For this experiment, we selected nanotube layers with the inner diameter of 35 nm, since they have demonstrated the highest IPCE in the whole spectral range (300-650 nm). One can see from Fig. 3 A and B that IPCE of CdS-coated TiO_2 heterostructures increased with increasing temperature of prior annealing of TiO_2 nanotube layers in the range of temperatures from 300 to 600 °C.
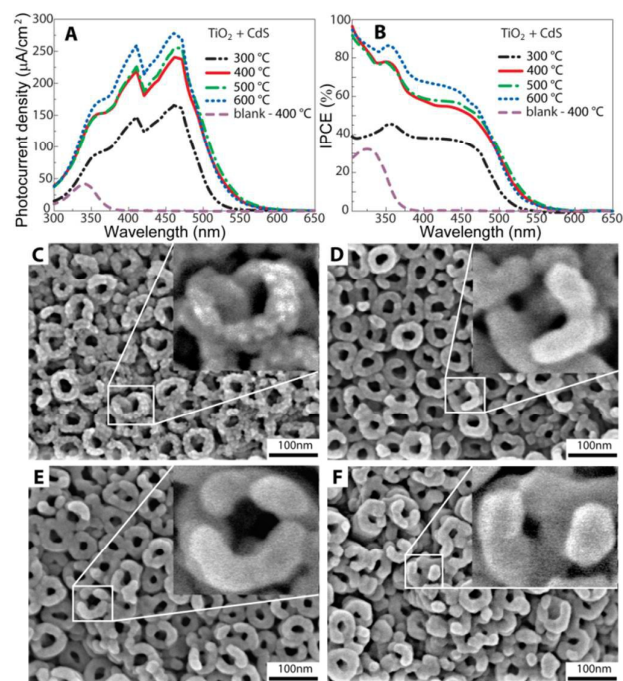

Fig. 3 A) photocurrent density B) incident photon-to-electron conversion efficiency (IPCE) recorded for of anatase TiO_2 nanotube layers with 35 nm inner diameter annealed at 300, 400, 500 and 600 °C and sensitized with crystalline CdS films by ALD. C) to F) represent top view SEM images of CdS-coated TiO_2 nanotube layers annealed at: C) 300 °C, D) 400 °C, E) 500 °C and F) 600 °C.

The enhancement in IPCE is not linear with rising temperature and can be divided into 3 steps. The most intensive improvement in IPCE was observed when TiO_2 nanotube layers were pre-annealed from 300 to 400 °C. Next, it seems that annealing of TiO_2 nanotube layers at 400 and 500 °C has a similar effect while annealing at 600 °C, which leads to the anatase to rutile transition,[29] adds further contribution to IPCE. In order to obtain a deeper understanding of this phenomenon, we collected FE-SEM top-view images of the CdS- coated TiO_2 nanotube layers (see Fig. 3 C to F) in combination with X-ray diffraction (see Fig. 4). At first sight, one can see that the level of TiO_2 nanotube layer coverage by CdS is noticeably different. While the TiO_2 nanotube layers pre-annealed at 300°C are decorated with CdS nanoparticles as demonstrated in Fig. 3C, a compact and uniform CdS crystalline coating was formed on TiO_2 nanotube layers pre-annealed at 400, 500 and 600 °C (see Fig. 3 D to F). These results indicate that the CdS deposition on TiO_2 nanotubes via ALD strongly depends on the TiO_2 crystallinity. In the case of TiO_2 nanotube layers pre-annealed at 300°C, the incubation time for the CdS nucleation seems to be longer than for all other samples pre-annealed at higher temperatures. As a consequence of that, these TiO_2 nanotube layers are only decorated by CdS nanoparticles leading to lower total mass of CdS and thus lower IPCE. Since it is evident from XRD that the background in the range of 2 theta from 10 to 22° has different shape for this particular TiO_2 nanotube layer pre-annealed at 300 °C indicating the presence of an amorphous phase, one may assume that the CdS nanoparticle growth can be attributed to the incomplete transformation of originally amorphous TiO_2 nanotubes to the anatase phase. On the other hand, TiO_2 nanotube layers pre-annealed at higher temperatures template the crystal growth of CdS which corresponds to the well evolved crystals. Overall, these findings corroborate well with literature that shows that different crystallinity of substrates used for ALD leads to different ALD deposition progress.[33,34]
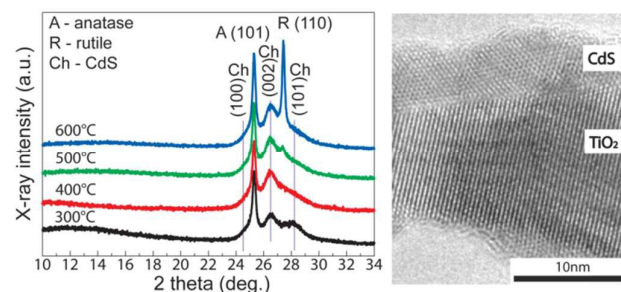

Fig. 4 Bragg diffractions of TiO_2 nanotube layers with 35 nm inner diameter annealed at 300, 400, 500 and 600 °C and sensitized with crystalline CdS films deposited by ALD (left panel). The HRTEM image of the TiO_2 nanotube layer pre-annealed at 400°C coated with CdS (right panel).

The templating effect is obvious as well from the XRD patterns and the HRTEM image. CdS crystallizes in the hexagonal phase within the space group $P6_3mc$[35] and lattice parameters a = 4.16 Å, c = 6.68 Å. Both the anatase and the rutile modifications

possess one cubic face with lattice parameters a = 3.784 Å (space group I4$_1$/amd)[36] and a = 4.594 Å (space group P4$_2$/mnm)[36] which results in lattice mismatches with CdS 10% and 10.4%, respectively. Since the lattice mismatch between CdS and TiO$_2$ phases is small, the nucleation and subsequent crystal growth can proceed fast. From XRD patterns, one can see that CdS crystallizes with the preferential orientation along the crystallographic plane (002) which is more pronounced with increasing the pre-annealing temperature of TiO$_2$ nanotube layers. This observation also supports the idea that fully crystalline TiO$_2$ nanotube layers pre-annealed at temperatures at/above 400 °C are suitable matrices for the ALD deposition of uniform CdS coatings.

Conclusions

We presented photo-electrochemical results for anodic TiO$_2$ nanotube layers grown with different diameter sizes (35, 56 and 95 nm) with a thickness of approx. 600 nm sensitized with 6 nm thick CdS coatings deposited by ALD. We found that the collected photocurrents increased approximately by a factor of 2 with downscaling of the TiO$_2$ nanotube diameter from 95 to 35 nm in the spectral range from 300 to 500 nm. The result perfectly coincides with the increased active surface area of TiO$_2$ nanotube layers in the same range of nanotube diameters. We also demonstrated the effect of annealing temperature of TiO$_2$ nanotube layers on the photocurrent generation of the CdS-coated TiO$_2$ nanotube layer photochemical cell. This study unequivocally showed that nanotube layers pre-annealed at temperatures higher than 400 °C generated higher photocurrent density in the spectral range from 350-550 nm than nanotube layers pre-annealed at 300 °C due to the presence of amorphous phase. Last but not least, we showed the added value of ALD for uniform coating of nanotube layers by functional secondary material.

Acknowledgements

Notes and references

1   M. A. Green, K. Emery, Y. Hishikawa, W. Warta and E. D. Dunlop, *Progress in Photovoltaics: Research and Applications,* 2016, **24**, 905-913.
2   D. E. Carlson and C. R. Wronski, *Appl. Phys. Lett.,* 1976, **28**, 671.
3   J. Britt and C. Ferekides, *Appl. Phys. Lett.,* 1993, **62**, 2851.
4   P. Jackson, D. Hariskos, E. Lotter, S. Paetel, R. Wuerz, R. Menner, W. Wischmann and M. Powalla, *Progress in Photovoltaics: Research and Applications,* 2011, **19**, 894-897.
5   T. K. Todorov, J. Tang, S. Bag, O. Gunawan, T. Gokmen, Y. Zhu, and D. B. Mitzi, *Adv. Energy Mater.*, 2013, **3**, 34-38.
6   B. O´Regan and M. Grätzel, *Nature*, 1991, **353**, 737-740.
7   A. Kojima, K. Teshima, Y. Shirai, and T. Miyasaka, *J. Am. Chem. Soc.* 2009, **131**, 6050–6051.
8   W.-T. Sun, Y. Yu, H.-Y. Pan, X.-F. Gao, Q. Chen and L.-M. Peng, *J. Am. Chem. Soc.* 2008, **130**, 1124–1125.
9   D. Zhao and Ch.-F. Yang, *Renewable and Sustainable Energy Reviews,* 2016, **24**, 1048–1059.
10 H. Wang, G. Wang, Y. Ling, M. Lepert, C. Wang, J. Z. Zhang, and Y. Li, *Nanoscale*, 2012, **4**, 1463-1466.
11 M. Liu, M. M. Johnston and H. J. Snaith, *Nature,* 2013, **501**, 395-398.
12 J. M. Macak, H. Tsuchiya, A. Ghicov, K. Yasuda, R. Hahn, S. Bauer and P. Schmuki, *Curr. Opin. Solid State Mater. Sci.* 2007, **11**, 3–18.
13 S. So, I. Hwang, and P. Schmuki, *Energy and Environ. Sci.,* 2015, **8**, 849-854.
14 W. S. Kim, Y. G. Jang, D. H. Kim, H. C. Kim and S. H. Hong, *CrystEngComm*, 2012,**14**, 4963-4966.
15 Y. J. Hwang, C. Hahn, B. Liu, P. Yang, *ACS Nano* 2012, **6**, 5060-5069.
16 X. Li, J. Yu, J. Low, Y. Fang, J. Xiao and X. Chen, *J. Mater. Chem. A*, 2015, **3**, 2485-2534.
17 H. Mirabolghasemi, N. Liu, K. Lee and P. Schmuki, *Chem. Commun.*, 2013, **49**, 2067-2069.
18 Z. Miao, D. Xu , J. Ouyang, G. Guo, X. Zhao and Y. Tang, *Nano Lett.*, 2002, **2**, 717-720.
19 X. F. Gao, H. B. Li, W. T. Sun, Q. Chen, F. Q. Tang and L. M. Peng, *J. Phys. Chem. C,* 2009, **113**, 7531-7535.
20 J. M. Macak, T. Kohoutek, L. Wang, R. Beranek, *Nanoscale*, 2013, **5**, 9541-9545.
21 M. Krbal, H. Sopha, V. Podzemna, S. Das, J. Prikryl and J. M. Macak, *J. Phys. Chem C,* 2017,**121**, 6065-6071.
22 J. A. Fernandes, P. Migowski, Z. Fabrim, A. F. Feil, G. Rosa, S. Khan, G. J. Machado, P. F. P. Fichtner, S. R. Teixeira, M. J. L. Santos and J. Dupont, *Phys.Chem.Chem.Phys.,*2014, **16**, 9148-9153.
23 S. Das, H. Sopha, M. Krbal, R. Zazpe, V. Podzemna, J. prikryl and J. M. Macak, ChemElectroChem, 2017, **4**, 495-499.
24 S. S. Kalanur, S. H. Lee, Y. J. Hwang and O.-S. Joo, *J. Photochem. Photobiol. A,* 2013, **259** 1– 9.
25 F. Tian, D. Hou, F. Hu, K. Xie, X. Qiao and D. Li, *Appl. Surf. Sci*, 2017, **391**, 295-302.
26 H. Cai, Q. Yang, Z. Hu, Z. Duan, Q. You, J. Sun, N. Xu and J. Wu, *Appl. Phys. Lett.* 2014, **104**, 053114.
27 R. Zazpe, M. Knaut, H. Sopha, L. Hromadko, M. Albert, J. Prikryl, V. Gärtnerova, J. W. Bartha, J. M. Macak, *Langmuir* 2016, **32**, 10551-10558.
28 R. Zazpe, J. Prikryl, V. Gärtnerova, K. Nechvilova, L. Benes, L. Strizik, A. Jäger, M. Bosund, H. Sopha and J. M. Macak, *Langmuir,* 2017, **33**, 3208-3216.
29 S. Das, R. Zazpe, J. Prikryl, P. Knotek, M. Krbal, H. Sopha, V. Podzemna and J. M. Macak, *Electrochimica Acta,* 2016, **213,** 452-459.
30 J. W. Zheng, A. Bhattcahrayya, P. Wu, Z. Chen, J. Highfield, Z. Dong and R. Xu, *J. Phys. Chem C* 2010, **114**, 7063-7069.
31 T. Umebayashi, T. Yamaki, H. Itoh and K. Asai, *Appl. Phys. Lett.* 2002, **81**, 454-456.
32 Y.-L. lee and Y.-S. Lo, *Adv. Funct. Mater.*, 2009, **19**, 604-609.
33 R. S. Pessoa, F. P. Pereira, G. E. Testoni, W. Chiappim, H. S. Maciel and L. V. Santos, *Journal of Integrated Circuits and Systems,* 2015, **10**, 38-42.
34 H.B.R. Lee and S. Bent, *Chem. Mater.*, 2012, **24**, 279-286
35 A. A. Andreev, M. F. Bulanyi, S. A. Golikov and L. A. Mozharovskii, *Russ. J. Inorg. Chem.*, 1995, **40**, 1039-1042.
36 D. W. Kim, N. Enomoto, Z. Nakagawa and K. Kawamura, *J. Am. Ceram. Soc.*, 1996, **79**, 1095-1099.